PHYSICAL REVIEW B VOLUME 47, NUMBER 20 15 MAY 1993-II

# Quantum Monte Carlo studies of binding energy and radiative lifetime of bound excitons in direct-gap semiconductors

A. C. Cancio and Yia-Chung Chang
*Department of Physics and Materials Research Laboratory, University of Illinois at Urbana-Champaign, Urbana, Illinois 61801*
(Received 30 November 1992)

We calculate the binding energy and the oscillator strength for radiative recombination of the bound exciton in direct-gap semiconductors in the spherical effective-mass approximation. The variational Monte Carlo method is used to evaluate the ground-state energy with a variational wave function that includes all pair correlations between particles. An importance-function Monte Carlo method is used to evaluate the corresponding optical-matrix element. We obtain variational energies for the donor bound exciton at all electron-hole mass ratios and recover about 60% of the experimental binding energy for various direct-gap semiconductors. The matrix element squared for the donor bound exciton in this model is twice as large as previous estimates, confirming the large disrepancy between the experimental and theoretical estimates of its radiative lifetime.

## I. INTRODUCTION

There is an extensive amount of experimental data from bound excitons (BE's) in direct-gap semiconductors—they have been observed in nearly all semiconductors of sufficient purity and at temperatures low enough for thermal stability.[1,2] They are a prominent feature of the photoluminescence spectra of direct-gap semiconductors, as the dominant channel of exciton decay is by radiative recombination at impurity sites. The strong and sharply defined photoluminescence lines of these localized states give much insight not only into the nature of these complexes, but also into the properties of specific impurities and the bulk crystal,[3] and they serve as a useful tool for characterizing residual impurities in ultrapure samples.[4]

Given the importance of BE photoluminescence, it has been of considerable interest to understand theoretically the ground-state and excited-state spectra as well as optical properties such as the radiative lifetime of these systems. Of the various processes that contribute to the lifetime of an exciton bound to a shallow impurity, that of radiative recombination has proven to be the dominant effect, due to a "giant" oscillator strength[5] resulting from the $k=0$ optical selection rule and the large spatial extent of these weakly bound systems. In particular, Auger recombination, in which the electron and hole recombine nonradiatively through a Coulomb interaction and deposit the remaining particle deep in the valence or conduction band, is greatly reduced by momentum conservation[6] and plays a noticeable role only with sufficiently deep traps or with indirect-gap materials. The bound exciton radiative lifetime was first estimated by Rashba and Gurgenishvili,[7] using a naive model of an exciton interacting with an impurity site through a $\delta$-function potential. Several authors have calculated the bound exciton ground state variationally with a variety of models, using the optimized variational wave function to calculate the ground-state bound exciton radiative oscillator strength. These include several based on simple models of acceptor or donor complexes[6,8] and a quantitative calculation using the Page-Fraser expansion form.[9]

There has also been ongoing experimental interest in the radiative lifetime of BE's in direct-gap semiconductors. The earliest measurements were carried out with an optical phase shift method[10–12] and produced lifetimes on the order of a nanosecond for both donor and acceptor complexes. These were the subject of some dispute, because of the method's inability to distinguish between any of several contributions to the BE decay rate such as the time of formation of the BE or long-lived anomalous decay processes. In addition, rather serious discrepancies with theoretically calculated donor BE decay times[8] left the field in an ambiguous state. In recent years, however, the increased sensitivity and resolution of photodetection devices and the use of mode-locked dye lasers has allowed the explicit time dependence of BE lines of specific impurity types to be measured, providing a measure of experimental control great enough to obtain lifetime data of a more definitive nature. To date, time decay studies exist for CdSe,[13] ZnSe,[14] ZnTe,[2] and GaAs,[15] providing a variety of examples for comparison to theory. In particular, studies have focused on the role of Auger recombination as a function of impurity energy,[2] and the effects of formation times a function of impurity concentration and excitation frequency.[13] These measurements for the most part confirm the existence of large experimental donor BE lifetimes and the dominant role of radiative decay for experimentally determined lifetimes. In addition, the role of thermal occupation of rotational states on the lifetimes of donor complexes in GaAs has been estimated by comparing the integrated absorption coefficient and lifetime.[15]

From a theoretical point of view, the bound exciton,

 

consisting of an electron-hole pair bound to a shallow impurity by screened Coulomb interactions, is an interesting few-body problem exhibiting a transition from an $H_2$ moleculelike system, to that of positronium hydride (PsH), to that resembling the $H^-$ ion as a function of changing electron-hole mass ratio. The need for an accurate wave function for all mass ratios is necessary for calculating a transition matrix element, in which defects in the trial wave function with small effect on the binding energy can be magnified into serious order-of-magnitude effects in the calculation of the lifetime.[8,16] The calculation of the bound exciton optical-matrix element is therefore a useful test of current models for Coulombic few-body systems. Quantitative variational calculations on the bound exciton to date have been done with Page-Fraser–type wave functions. The binding energy[17] and radiative oscillator strength[9] have been calculated with a 35-term wave function which was subsequently redone with 70 parameters to estimate BE radii,[18] and a 105-term calculation exists for PsH.[19] Unfortunately, the method involves an expansion about a model that is accurate only for acceptor complexes, and is inefficient for the electron-hole mass ratios typical of donor complexes. With the large numbers of expansion terms necessary for convergence in this case, it sheds little light onto the underlying physics of the system.

We approach the calculation of the binding energy and optical-matrix element of the bound exciton with a variational Monte Carlo method (VMC) using a correlated trial wave function. Quantum Monte Carlo (QMC) methods[20] have been employed in the study of several important many-body problems, such as the electron gas,[21,22] liquid and solid He,[23] and to obtain nearly exact ground-state energies for small atoms and molecules.[24] In particular they have been used in standard ground-state variational calculations to systematically improve trial wave functions for many-body systems with much fewer restrictions on variational form than are feasible with conventional methods. As a result, it is possible to obtain with fairly simple and compact wave functions ground-state energies for small atoms and molecules comparable in accuracy to the most extensive of configuration-interaction bases.[25,26] The particular advantage of the method is that correlated wave functions can be derived from physically motivated arguments rather than brute force expansion and thus provide physical insight into the nature of interparticle correlations as well as accurate expectation values. The bound exciton, as an analog to small atomic or molecular systems in the effective-mass approximation, is a natural candidate for this kind of approach, and effective-mass models of biexcitons[27] and complexes of several excitons[28] have been successfully studied with QMC approaches.

The current paper is presented as follows. Section II describes the theory of the ground-state and optical properties of the bound exciton and the correlated trial wave function used in the VMC calculation. Section III gives an overview of the VMC method and describes in detail the method used to calculate the optical-matrix element. Our results are presented in Sec. IV along with a discussion comparing the various theoretical approaches that have been used to date. The data are compared to experimental lifetime data in Sec. V and a summary presented in the conclusion, Sec. VI.

## II. THEORY

### A. Hamiltonian

We consider the ground state of a system consisting of an electron-hole pair bound to a positively charged donor ion and a weakly bound donor electron in the case of a donor BE or a negatively charged acceptor ion plus hole in the acceptor case. Focusing on the role of interparticle correlations in the BE, we use the spherical effective-mass model to describe single-particle dispersion relations, parametrizing the kinetic energy of electrons in the vicinity of the conduction-band minimum and of holes near the valence-band maximum by a spherical effective electron mass $m_e$ and hole mass $m_h$. Particles interact with each other and with the impurity ion through Coulomb interactions screened by the static dielectric constant of the crystal $\epsilon_0$. The bound exciton in this approximation is described by an effective Hamiltonian for a system of charged particles which, with the choice of suitable units, depends only on the charge of the ion and the electron-hole mass ratio $\sigma$. Taking the donor bound exciton for specificity, using natural units of donor radius $a_D=\hbar^2/(m_e e^2/\epsilon_0)$ and donor Rydberg $E_D=m_e e^4/2\epsilon_0^2\hbar^2$, the Hamiltonian of the system can be written as

$$H=\sum_{i=1}^{2}\left[-\nabla_i^2-\frac{2Z_I}{r_i}\right]+\left[-\sigma\nabla_3^2+\frac{2Z_I}{r_3}\right]+\frac{2}{r_{12}}-\frac{2}{r_{13}}-\frac{2}{r_{23}}\,, \tag{1}$$

where $\mathbf{r}_1$ and $\mathbf{r}_2$ are electron coordinates, and $\mathbf{r}_3$ is the coordinate of the hole. $Z_I$ is the charge of the donor ion, equal to $+1$ for the case of a singly ionized donor. Within the spherical effective-mass approximation, the Hamiltonian for an acceptor BE or $A^0X$ with electron-hole mass ratio $\sigma$ is equal to that of a donor BE or $D^0X$ with mass ratio $1/\sigma$ with the reversal of the signs of charges. In particular, the ground-state energy of the $A^0X$ with mass ratio $\sigma$ is equal to that of the $D^0X$ for a mass ratio $1/\sigma$: $E_{A^0X}(\sigma)=E_{D^0X}(1/\sigma)$.

The eigenstate of the crystal associated with this electron-hole system is given by the product of the wave function $F(\mathbf{r}_1,\mathbf{r}_2,\mathbf{r}_3)$ obtained from the effective-mass Hamiltonian and the Bloch functions $|j_i\mu_i\rangle$ for electrons and holes at the conduction- and valence-band edges, respectively. The Bloch state for the conduction-band minimum is twofold degenerate with spin $\frac{1}{2}$; the valence-band maximum is fourfold degenerate obeying approximately a $j=\frac{3}{2}$ spin symmetry. The total wave function is an appropriate linear combination of degenerate single-particle Bloch state products forming an eigenstate of the total angular momentum of the system and its projection upon the $z$ axis, with eigenvalues $J$ and $M$,

$$\psi_{\mathrm{BE}}^{JM}=\sum_{\mu_1,\mu_2,\mu_3} C_{j_1\mu_1 j_2\mu_2 j_3\mu_3}^{JM} \times F(\mathbf{r}_1,\mathbf{r}_2,\mathbf{r}_3)|j_1\mu_1\rangle|j_2\mu_2\rangle|j_3\mu_3\rangle \ . \quad (2)$$

Ignoring the potentially significant effects of the coupling of the hole envelope angular momentum with its Bloch spin and other such complications, the main contribution of the complex valence band in this model is the large degeneracy it gives the bound exciton ground state, fourfold for $D^0X$ and twelvefold for $A^0X$, an important consideration in determining optical transition rates.

The bound exciton ground state can be understood qualitatively from several limiting cases of the Hamiltonian as a function of electron-hole mass ratio $\sigma$. At $\sigma=0$, i.e., the case of infinite hole mass, the Hamiltonian reduces to that of the hydrogen molecule $H_2$, with ground-state energy $2.346E_D$ and bond length between exciton and donor of $1.4a_D$. At the other extreme of zero hole mass, the kinetic energy of the hole forces it away from the donor, leaving a core consisting of the much heavier electrons bound to the donor in a $H^-$-like complex. The core then acts approximately as a single particle with net charge $-e$ binding the hole in a $1s$ hydrogen orbital. The intermediate regime is characterized by the case of equal electron and hole masses, in which case the Hamiltonian is equivalent to that of positronium hydride, i.e., a positron-electron complex bound to a hydrogen atom. This region is much harder to treat theoretically, as there is no simple way to decouple the behavior of individual particles, and many-body correlations are important.[17,19]

### B. Variational wave function

We have chosen a form of trial wave function that provides an accurate ground-state energy for both the $H_2$-like and $H^-+h$-like regimes, taking interparticle correlations into account in a straightforward fashion. In general terms it can be expressed as

$$\psi_T(\mathbf{r}_1,\mathbf{r}_2,\mathbf{r}_3)=\tfrac{1}{2}(1+P_{12})f_{ei}^{\mathrm{in}}(r_1)f_{ei}^{\mathrm{out}}(r_2)f_{ee}(r_{12}) \times f_{eh}^{\mathrm{out}}(r_{13})f_{eh}^{X}(r_{23})f_{hi}(r_3) \ , \quad (3)$$

where $f_{ei}^{\mathrm{in}}$, $f_{ei}^{\mathrm{out}}$, and $f_{hi}$ are correlation functions describing, respectively, an inner electron orbital, an outer electron orbital, and a hole orbital about the ion; $f_{eh}^{X}$ and $f_{eh}^{\mathrm{out}}$ are an inner excitonlike and a weak outer electron-hole correlation function; and $f_{ee}$ is an electron-electron correlation function; $P_{12}$ is the electron permutation operator. This wave function reduces to a generalized Heitler-London form with additional pair correlations in the $\sigma=0$ limit and to a similar generalization of Chandresekhar's form for the $H^-$ ion[16] in the opposite limit.

The behavior of the correlation functions $f_{\alpha\beta}(r)$ at short distances can be largely optimized by satisfying the cusp conditions of the wave function that arise from the singular behavior of the Coulomb interaction $\sim 1/r$ as $r$ tends to zero.[21] For interparticle distances larger than an exciton radius, one expects that most of the correlation functions show the effects of screening by other particles, while $f_{ei}^{\mathrm{in}}$ and $f_{eh}^{X}$ stay fairly close to the donor and exciton $1s$ states, respectively.

To generate the correlation functions, we use a generalized two-body Schrödinger equation for each kind of particle-particle interaction and solve for $f_{\alpha\beta}(r)$ numerically,

$$H_{\alpha\beta}f_{\alpha\beta}(r)=\lambda_{\alpha\beta}(r)f_{\alpha\beta}(r) \ ,$$
$$H_{\alpha\beta}=-\frac{1}{\mu_{\alpha\beta}}\nabla^2+\frac{2Z_\alpha Z_\beta}{r} \ , \quad (4)$$
$$\lambda_{\alpha\beta}(r)=\Lambda_{\alpha\beta}\exp(-r^2/r_{\mathrm{sc}}^2) +\exp(k_{\alpha\beta}r)[H_{\alpha\beta}\exp(-k_{\alpha\beta}r)] \times[1-\exp(-r^2/r_{\mathrm{sc}}^2)] \ .$$

$\Lambda_{\alpha\beta}$ is determined by requiring that $\lim_{r\to 0} rf_{\alpha\beta}(r)=0$ and the $k_{\alpha\beta}$ for the different types of interactions and the screening length $r_{\mathrm{sc}}$ are variational parameters. The correlation functions thus generated satisfy the cusp condition for the bare Coulomb interaction at $r=0$; they approach the asymptotic form $\exp(-k_{\alpha\beta}r)$ for distances much larger than $r_{\mathrm{sc}}$. Other asymptotic forms were also used, notably for the electron-electron correlation function, for which the forms $1+br$ or $\exp[br/(1+cr)]$ gave modest improvements to the variational energy.

### C. Optical properties

Using the generalization of Fermi's golden rule and Einstein's arguments of detailed balance to optical processes in a dielectric material, the radiative lifetime of a bound exciton is given by[29]

$$\frac{1}{\tau_R}=\frac{2e^2\omega^2 n}{c^3 m}f_{\mathrm{emission}} \ . \quad (5)$$

Here, $n$ is the index of refraction, $\hbar\omega$ is the transition energy, and $f$ is the oscillator strength of the transition. In the effective-mass approximation, the total oscillator strength is given by[8]

$$f_{\mathrm{emission}}=\frac{P^2}{3\hbar\omega}|\langle I|F\rangle|^2 \ , \quad (6)$$

$$P^2=\frac{2}{m}|\langle S|P_x|X\rangle|^2 \ . \quad (7)$$

Here, $|\langle S|P_x|X\rangle|^2$ is the dipole matrix element over one unit cell between the Bloch state of the conduction-band minimum $|S\rangle$ and a Bloch state $|X\rangle$ of the degenerate valence-band maximum with angular momentum $L_x=1$. $|\langle I|F\rangle|^2$ is an overlap integral between the effective-mass envelopes of the initial state of the system, assumed to be in the bound exciton ground state, and the final state of the system, a donor or acceptor in its ground state,

$$\langle I|F\rangle=\int d^3\mathbf{r}_1 d^3\mathbf{r}_2 d^3\mathbf{r}_3 \phi_I(\mathbf{r}_1,\mathbf{r}_2,\mathbf{r}_3)\delta(\mathbf{r}_2-\mathbf{r}_3)\phi_F(\mathbf{r}_1) \ . \quad (8)$$

The impurity ground state is a $1s$ hydrogen orbital $\phi_F(r)=\exp(-r)/\sqrt{\pi}$ and the $\delta$ function is derived from

the requirement that the recombining electron and hole occupy the same unit cell. The intrinsic band-to-band matrix element $P^2$ includes averaging over the vector components of the momentum operator $\mathbf{P}$, averaging over the Bloch states of the initial degenerate bound exciton ground state, and summing over the degeneracies of the ground state of the donor or acceptor. Ignoring fine structure due to crystal-field effects, the sum over all possible decay channels gives an expression independent of crystal structure (wurtzite or zinc blende) or the type of impurity involved.[8]

The condition of detailed balance ties the value of the radiative lifetime to that of measurements of the associated absorption process. In particular, the integrated absorption strength of the impurity to bound exciton transition is given by[15,29]

$$\int \sigma(E)dE = \frac{2\pi^2 e^2 \hbar}{mcn} f_{\text{abs}} , \tag{9}$$

where

$$f_{\text{abs}} = \frac{g_{\text{BE}}}{g_I} f_{\text{emission}} , \tag{10}$$

taking into account the exchanged roles of the impurity state with degeneracy $g_I$ and bound exciton state with degeneracy $g_{\text{BE}}$ as the initial and final states of the absorption process.

A qualitative understanding of the effective-mass envelope contribution to the optical-matrix element can be derived from a simple model of the bound exciton as an exciton weakly coupled to the donor through an effective interaction acting upon its center of mass.[7,8] The corresponding wave function is

$$\psi = \tfrac{1}{2}(1+P_{12})\phi_D(r_1)\phi_X(r_{23})F(R_{23}) , \tag{11}$$

where $\phi_D$ and $\phi_X$ are the donor and exciton ground states, and $F$ describes the correlation of the center-of-mass $R_{23}$ of the exciton with the donor and $P_{12}$ is the electron permutation operator. The effective-mass overlap integral, [Eq. (8)], is given approximately by

$$|\langle I|F\rangle|^2 = |\phi_X(0)|^2 \left| \int d^3r\, F(r) \right|^2 , \tag{12}$$

including only those processes in which the exciton electron recombines.[30] The matrix element squared is the probability, $\sim 1/a_X^3$, that the electron and hole in an exciton are at the same point in space, multiplied by the integral over the exciton-donor correlation function squared. The latter, having dimensions of volume, can be considered a measure of the volume within which the center of mass of the exciton is confined by the impurity potential. This model suggests that the contribution of the spatially extensive effective-mass envelope to the oscillator strength measured relative to that of a given unit cell of volume $\Omega$ is determined by a competition between two effects—the small probability $\sim\Omega/a_X^3$ that the electron and hole in a Wannier exciton will occupy the same unit cell, and the large number of unit cells, as measured by $|\int F(r)d^3r|^2/\Omega$, on which the weakly bound exciton can recombine. The resulting overlap matrix element can show a wide range of behavior, with very large overlaps for $\sigma < 1$ where both the electron-hole overlap and the spatial extent of the exciton center-of-mass envelope are large, to vanishingly small overlaps for $\sigma > 1$ where the average electron-hole separation tends to infinity compared to its center of mass.

## III. VARIATIONAL MONTE CARLO METHOD

### A. Ground-state expectation values

The variational Monte Carlo method (VMC) is based on an algorithm devised by Metropolis *et al.*[31] for calculating integrals of the form

$$\langle O \rangle = \frac{\int dR\, |\psi(R)|^2 O(R)}{\int dR\, |\psi(R)|^2} , \tag{13}$$

where $R$ is the coordinate of a $3N$-dimensional configuration space $\{\mathbf{r}_1, \mathbf{r}_2, \ldots, \mathbf{r}_N\}$, and $dR$ is the volume element for integration over the configuration space $d^3r_1 d^3r_2 \cdots d^3r_N$. The key to the method is a simple and efficient algorithm for generating a random series of points $\{R_i\}$, with a probability distribution given by

$$P(R) = |\psi(R)|^2 \Big/ \int dR\, |\psi(R)|^2 . \tag{14}$$

Given a set of $M$ independent points sampled from this distribution, the integral can then be estimated statistically as

$$\bar{O} = \frac{1}{M} \sum_{i=1}^{M} O(R_i) \tag{15}$$

with a statistical error of order $\sigma_o / M^{-1/2}$, where

$$\sigma_O = \sqrt{\langle |O(R) - \langle O \rangle|^2 \rangle} \tag{16}$$

is the standard deviation of the function $O(R)$ from its mean value. The method is most useful for multidimensional integrals, since the error in an $M$-point sample is independent of dimension, whereas other numerical methods will have in general some power-law dependence.

The details of the Metropolis method are discussed in the literature,[20,32] and it is important only to note that the algorithm's success lies in its sampling the probability function $P(R)$ without knowledge of the normalization of the wave function used to generate it, making the calculation of expectation values of sophisticated many-body wave functions possible. At the same time, it is not possible to calculate directly from the statistical information generated by the method the normalization of $\psi$ or other integrals not of an expectation value form.

A variational calculation involves the calculation of the energy expectation value $E(\alpha)$ of a trial wave function $\psi_T(R,\alpha)$ parametrized by a set of variational parameters $\alpha = (\alpha_1, \alpha_2, \ldots, \alpha_M)$,

$$E(\alpha) = \frac{\int dR\, \psi^*(R;\alpha) H \psi(R;\alpha)}{\int dR\, |\psi(R;\alpha)|^2} . \tag{17}$$

The variational energy can be easily evaluated by the Metropolis scheme as the expectation value of a local energy function

$$E(R;\alpha)=\psi^{-1}(R;\alpha)(H\psi(R;\alpha)) . \tag{18}$$

The calculation of the energy expectation value is particularly robust since choosing a good trial wave function not only results in a close upper bound to the ground-state energy but also in the reduction of the statistical error of its estimation, since the deviation of the local energy from its average $E(R,\alpha)-\langle E\rangle$ vanishes as the trial wave function $\psi(R,\alpha)$ tends to an eigenfunction of the system.

The optimal set of variational parameters $\alpha$ can be accurately determined by using correlated estimates.[20,26] This method is based on the observation that a set of configurations $\{R_i\}$ sampled from a trial wave function evaluated with a certain set of variational parameters $\alpha$ can be used to calculate the variational energy for a wave function with a different set of parameters $\alpha+\delta\alpha$ by means of a reweighting formula

$$\bar{E}(\alpha+\delta\alpha)=\frac{\frac{1}{M}\sum_{i=1}^{M} E(R_i,\alpha+\delta\alpha)\left|\frac{\psi(R_i,\alpha+\delta\alpha)}{\psi(R_i,\alpha)}\right|^2}{\frac{1}{M}\sum_{i=1}^{M}\left|\frac{\psi(R_i,\alpha+\delta\alpha)}{\psi(R_i,\alpha)}\right|^2} . \tag{19}$$

Repeated correlated estimates generate from a given random walk an estimate function $\bar{E}(\alpha)$ of the trial energy versus its variational parameters. With judicious avoidance of bias effects that can arise for too small a sample size $M$ or too large a variation $\delta\alpha$,[20] the shape of this function matches that of the analytic variational energy $E(\alpha)$ to a greater precision than the actual value of the function at any given point. This approach can be combined with standard function optimization techniques to locate and map out the minimum of the variational energy.

### B. Optical-matrix element

The overlap matrix element for radiative recombination

$$|\langle I|F\rangle|^2=\frac{\left|\int d^3\mathbf{r}_1 d^3\mathbf{r}_2\psi(\mathbf{r}_1,\mathbf{r}_2,\mathbf{r}_2)\phi_{D^0}(\mathbf{r}_1)\right|^2}{\int d^3\mathbf{r}_1 d^3\mathbf{r}_2 d^3\mathbf{r}_3|\psi(\mathbf{r}_1,\mathbf{r}_2,\mathbf{r}_3)|^2} \tag{20}$$

is not directly calculable from a Metropolis Monte Carlo calculation. There are at least two separate calculations to be made, one to perform the overlap matrix element over a restricted configuration space with the hole coordinate $\mathbf{r}_3$ equal to the electron coordinate $\mathbf{r}_2$, and one to calculate the normalization of the bound exciton wave function, which requires a sampling over the full configuration space. Each must in addition be recast in the form of Eq. (13) in order to apply a Monte Carlo method to their evaluation, and some care must be taken to adopt an effective sampling distribution.

To calculate the normalization of the wave function $\psi$,

$$N[\psi]=\int d^3\mathbf{r}_1 d^3\mathbf{r}_2 d^3\mathbf{r}_3|\psi(\mathbf{r}_1,\mathbf{r}_2,\mathbf{r}_3)|^2 , \tag{21}$$

with the Monte Carlo method, the problem is recast as the calculation of the ratio of normalization integrals of two wave functions,

$$\frac{N[\psi_I]}{N[\psi]}=\frac{\int d^3\mathbf{r}_1 d^3\mathbf{r}_2 d^3\mathbf{r}_3|\psi_I(\mathbf{r}_1,\mathbf{r}_2,\mathbf{r}_3)|^2}{\int d^3\mathbf{r}_1 d^3\mathbf{r}_2 d^3\mathbf{r}_3|\psi(\mathbf{r}_1,\mathbf{r}_2,\mathbf{r}_3)|^2} . \tag{22}$$

This ratio can be estimated by a standard Metropolis Monte Carlo algorithm by sampling $|\psi|^2$ and calculating the expectation value

$$\left\langle\left|\frac{\psi_I}{\psi}\right|^2\right\rangle=\frac{\int d^3\mathbf{r}_1 d^3\mathbf{r}_2 d^3\mathbf{r}_3\left|\frac{\psi_I(\mathbf{r}_1,\mathbf{r}_2,\mathbf{r}_3)}{\psi(\mathbf{r}_1,\mathbf{r}_2,\mathbf{r}_3)}\right|^2|\psi(\mathbf{r}_1,\mathbf{r}_2,\mathbf{r}_3)|^2}{\int d^3\mathbf{r}_1 d^3\mathbf{r}_2 d^3\mathbf{r}_3|\psi(\mathbf{r}_1,\mathbf{r}_2,\mathbf{r}_3)|^2} . \tag{23}$$

The importance wave function $\psi_I$ is chosen to be close to $\psi$ while remaining simple enough in form for its normalization to be calculated by standard analytical or numerical methods. The normalization of the Monte Carlo trial wave function $\psi$ is then obtained from the product of the importance wave-function normalization and the Monte Carlo estimate of the ratio of the two normalizations,

$$N[\psi]=\left\langle\left|\frac{\psi_I}{\psi}\right|^2\right\rangle^{-1}N[\psi_I] . \tag{24}$$

The Monte Carlo estimate is thus essentially a calculation of the correction to a first guess at the normalization of $\psi$, $N[\psi_I]$. The variance of the Monte Carlo correction is consequently reduced in proportion to how well the first-guess importance function approximates the form of the trail wave function. In particular, the relative variance of the Monte Carlo estimate, as defined by

$$f=\left\langle\left|\frac{\psi_I}{\psi}\right|^4\right\rangle\Big/\left\langle\left|\frac{\psi_I}{\psi}\right|^2\right\rangle^2-1 , \tag{25}$$

goes to zero as the importance wave function $\psi_I(R)$ approaches $\psi(R)$ for all $R$. In principle, this property of $f$ could be used to solve variationally for the parameters of any given simple form of $\psi_I$ that produces the lowest variance in the Monte Carlo estimate; in practice, common sense guesswork can provide importance wave functions of sufficiently small variance without too much effort.

The overlap integral is calculated in much the same way, with slightly different choice of sampling function. It is recast as

$$O[\psi]=\left\langle\frac{\psi_I}{\psi}\right\rangle_O^{-1} O[\psi_I]\ , \tag{26}$$

where

$$O[\psi]=\int d^3\mathbf{r}_1 d^3\mathbf{r}_2 \psi(\mathbf{r}_1,\mathbf{r}_2,\mathbf{r}_2)\phi_{D^0}(\mathbf{r}_1) \tag{27}$$

and

$$\left\langle\frac{\psi_I}{\psi}\right\rangle_O=\frac{\int d^3\mathbf{r}_1 d^3\mathbf{r}_2\left[\frac{\psi_1(\mathbf{r}_1,\mathbf{r}_2,\mathbf{r}_2)}{\psi(\mathbf{r}_1,\mathbf{r}_2,\mathbf{r}_2)}\right]\psi(\mathbf{r}_1,\mathbf{r}_2,\mathbf{r}_2)\phi_{D^0}(\mathbf{r}_1)}{\int d^3\mathbf{r}_1 d^3\mathbf{r}_2\psi(\mathbf{r}_1,\mathbf{r}_2,\mathbf{r}_2)\phi_{D^0}(\mathbf{r}_1)}\ . \tag{28}$$

The brackets $\langle\ \rangle_O$ denote an expectation value with respect to a probability distribution

$$P_O(\mathbf{r}_1,\mathbf{r}_2)=\psi(\mathbf{r}_1,\mathbf{r}_2,\mathbf{r}_2)\phi_{D^0}(\mathbf{r}_1)\ . \tag{29}$$

Since $\psi$ and $\phi_{D^0}$ are both spatially symmetric ground states, their product $P_O$ is greater than or equal to zero for all $\mathbf{r}_1$ and $\mathbf{r}_2$ and thus is a well-defined probability distribution that can be sampled by Monte Carlo methods.

The method outlined above should provide the same value of the matrix element

$$\langle I|F\rangle=O[\psi]\Big/\left[N[\psi]\times\int d^3r|\phi_{D^0}(\mathbf{r})|^2\right]^{1/2}, \tag{30}$$

independent of the importance function used to filter out statistical noise; this reproducibility property is a useful check of one's computer code. At the same time, the quality of the estimate crucially depends on the quality of the importance function; an importance function that does not approximate the trial function sufficiently may produce a standard deviation several times larger than the expectation value itself, and thus prove unreliable.

We tried two different importance functions for the Monte Carlo calculation of the overlap integral. One was a generalized Hartree Fock form best suited for the $H^-$-type complex,

$$\psi_1(\mathbf{r}_1,\mathbf{r}_2,\mathbf{r}_3)=\tfrac{1}{2}[\exp(-k_1r_1-k_2r_2)+\exp(-k_2r_1-k_1r_2)]\exp(-\gamma r_3)\ , \tag{31}$$

another chosen to be fairly accurate for the $H_2$ limit,

$$\psi_2(\mathbf{r}_1,\mathbf{r}_2,\mathbf{r}_3)=\tfrac{1}{2}[\exp(-k_1r_1-k_2r_2-k_3r_{13}-k_4r_{23})+\exp(-k_2r_1-k_1r_2-k_4r_{13}-k_3r_{23})]f_{hi}(r_3)\ . \tag{32}$$

As shown in Fig. 2, the numerical hole-ion correlation $f_{hi}$ is flexible enough to interpolate over all electron-hole mass ratios, and thus is a natural choice for use in the importance function. Using this form, the normalization and overlap matrix elements reduce to a linear combination of numerically calculable one-dimensional integrals over the hole-ion correlation functions.

## IV. RESULTS

### A. Bound-exciton ground state

Table I shows the ground-state energy of the bound exciton, and average particle radii and interparticle distances. The binding energy with respect to dissociating an exciton from the complex is plotted in Fig. 1 along with results of the 35-term Page-Fraser variational wave function of Stebe and Munschy,[17] and a 105-term Page-Fraser calculation at $\sigma=1$.[19]

We can compare these results to those of the various limiting cases of the bound exciton to estimate how well our variational theory recovers the ground-state bound exciton binding energy. An adiabatic calculation of the $H_2$ molecule obtained by setting the hole-ion correlation in Eq. (3) to a $\delta$ function and corresponding to the $\sigma=0$ limit of the bound exciton gives an energy $E(\sigma)/\mathrm{Ry}$ of $-2.3360(10)+0.80(10)\sqrt{\sigma}$ with a bond length of $1.401(15)a_B$ as compared to the exact result of $-2.347+0.584\sqrt{\sigma}$ and 1.40.[33,34] The adiabatic scaling behavior obtained by extrapolating from our $\sigma>0$ data also agrees with these results. For the hydrogen ion $H^-$ which corresponds to the $\sigma\to\infty$ limit in Fig. 1, we obtain a best value for the ground-state energy of

TABLE I. $D^0X$ ground-state properties: average electron-ion, hole-ion, electron-electron, and hole-electron distances as a function of electron-hole mass ratio $\sigma$ in units of $a_D$; ground-state energy $E$, standard deviation of energy $\sigma_E$, and binding energy $W$ in units of the donor Rydberg $E_D$. Errors in the last digits are shown in parentheses. Bottom line using adiabatic wave function.

| $\sigma$ | $r_{ei}$ | $r_{hi}$ | $r_{ee}$ | $r_{eh}$ | $E$ | $\sigma_E$ | $W$ |
|---|---|---|---|---|---|---|---|
| 0.02 | 1.656(07) | 1.6087(26) | 2.329(06) | 1.6668(26) | −2.2328(08) | 0.354 | 0.2524 |
| 0.05 | 1.721(27) | 1.754(36) | 2.437(25) | 1.767(20) | −2.1654(15) | 0.345 | 0.2130 |
| 0.10 | 1.822(07) | 1.989(06) | 2.617(11) | 1.930(05) | −2.0830(23) | 0.341 | 0.1739 |
| 0.20 | 1.946(20) | 2.301(25) | 2.854(35) | 2.181(20) | −1.9638(21) | 0.371 | 0.1305 |
| 0.50 | 2.189(19) | 2.968(34) | 3.323(35) | 2.729(25) | −1.7528(13) | 0.263 | 0.0861 |
| 1.00 | 2.392(05) | 3.816(29) | 3.758(33) | 3.563(23) | −1.5656(10) | 0.215 | 0.0656 |
| 2.00 | 2.513(30) | 5.08(06) | 4.01(05) | 4.91(04) | −1.3905(07) | 0.171 | 0.0572 |
| 10.00 | 2.692(04) | 16.68(18) | 4.29(08) | 16.73(18) | −1.1456(06) | 0.124 | 0.0547 |
| 100.00 | 2.671(29) | 147.(11) | 4.35(05) | 147.(11) | −1.0636(06) | 0.088 | 0.0537 |
| 100.00 | 2.635(22) | 149.0(09) | 4.27(04) | 149.0(13) | | | |

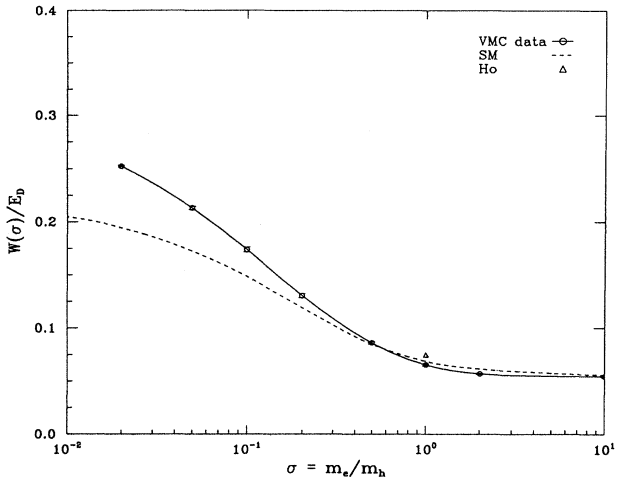


FIG. 1. Binding energy of the donor bound exciton in units of the donor Rydberg $E_D$, as a function of electron-hole mass ratio $\sigma$. Circles with error bars refer to the present calculation, the dotted line to the 35-parameter variational calculation of Stebe and Munschy, Ref. 17, the triangle at $\sigma=1$ to the 105-parameter calculation for PsH by Ho (Ref. 19). Acceptor bound exciton results can be obtained by $E_{A^0X(\sigma)}=E_{D^0X(1/\sigma)}$.

$-1.0540(5)$ Ry as compared with the exact value of $-1.0555$ Ry.[35]

The $\sigma=1$ case provides the strongest test of the accuracy of our variational model since no adiabatic approximation can be used to separate electron and hole behavior, and thus correlations between all particles will be important. Our fairly simple variational wave function recovers nearly 90% of the binding energy as compared to the best known variational result of 0.075 Ry for the equivalent system of positronium hydride.[19] Given similar agreement with nearly exact results at the special points of $\sigma=0$ and $\infty$, we expect our variational results to be within 5–15 % of the correct spherical effective-mass binding energy for all mass ratios.

Table II shows optimized variational parameters for the $D^0X$ trial wave function as a function of electron-hole mass ratio $\sigma$. The inner electron donor orbital $f_{ei}^{\rm in}$ has an exponential factor $k_{ei}^{\rm in}$ that is close to the donor $1s$ state value of 1 for all mass ratios. This strong correlation of the inner orbital with the donor ion leads to the small binding energy observed, the outer particles bound as a result of imperfect screening and polarization of the donor electron. The excitonic correlation function which describes the correlation between the outer electron and the hole is parametrized by the factor $k_{eh}^{X}$. It is close to what one would expect for a free exciton $1/(1+\sigma)$ for $\sigma=0.1$ but diminishes to only one-half that of the exciton for $\sigma=10$, and is small beyond the resolution of statistical error at $\sigma=100$. Such behavior indicates a picture in which for low $\sigma$ the hole binds strongly to the outer electron as an exciton which then interacts to a lesser extent with the donor. As the hole mass becomes lighter and its radius grows larger, the hole sees the $D^-$ core more as a point charge centered at the ion site, and electron-hole correlations gradually disappear. The crossover ratio of $\sigma=10$ at which the correlation between outer electron and hole has dropped to one-half that of a free exciton corresponds roughly to the mass ratio $\sigma=17$ at which the energy of ionization of the hole with respect to the $D^-$ core has become smaller than the exciton binding energy.

The hole-ion orbital is particularly sensitive to the change in character of the bound exciton as a function of mass ratio. In Fig. 2, the hole-ion orbital $f_{hi}$ for several mass ratios is plotted as a function of hole distance from the ion $r_{hi}$. For each case it varies from repulsive behavior near the ion characterized by the cusp condition at $r_{hi}=0$, to an attractive correlation with the ion caused by the attractive mean field of the interlying electrons, with the transition occurring roughly at $a_D$, set by the variational screening radius $r_{\rm sc}$. In the low-mass-ratio regime, it resembles the correlation between ions in the $H_2$ molecule, being sharp and peaked near the average hole radius. In the opposite limit, at mass ratio $\sigma=10$, it approaches an exponential $1s$ form typical of a hydrogenic orbit. The $\sigma=1$ orbital shows an intermediate regime

TABLE II. Optimized variational parameters for the bound exciton trial wave function as function of electron-hole mass ratio $\sigma$. Long-range decay parameters for pair-correlation functions $k_{\alpha\beta}$ are given in units of inverse donor radius $a_D^{-1}$, the screening length $r_{sc}$ in units of $a_D$. The electron-electron parameter refers to a long-range form of $1+b_{ee}r$. $k_{hI}^{*}=k_{eh}^{X}+k_{eh}^{\rm out}+k_{hI}$ is the exponential parameter for the adiabatic hole $1s$ orbital in the large-$\sigma$ limit, and $k_{eh}^{X}(1+\sigma)$ gives the ratio of the bound to free exciton variational parameters. Bottom line for adiabatic wave function.

| $\sigma$ | $k_{eI}^{\rm out}$ | $k_{eI}^{\rm in}$ | $k_{hI}$ | $b_{ee}$ | $k_{eh}^{\rm out}$ | $k_{eh}^{X}$ | $r_{sc}$ | $k_{hI}^{*}\sigma$ | $k_{eh}^{X}(1+\sigma)$ |
|---|---|---|---|---|---|---|---|---|---|
| 0.02 | 0.257 | 1.009 | 1.830 | 0.240 | 0.235 | 0.989 | 1.15 | | 1.009 |
| 0.05 | 0.252 | 1.008 | 1.139 | 0.208 | 0.199 | 0.953 | 1.21 | | 1.001 |
| 0.10 | 0.264 | 1.000 | 0.752 | 0.199 | 0.168 | 0.864 | 1.34 | | 0.950 |
| 0.20 | 0.316 | 0.988 | 0.481 | 0.232 | 0.134 | 0.756 | 1.49 | | 0.907 |
| 0.50 | 0.337 | 0.987 | 0.238 | 0.192 | 0.089 | 0.585 | 1.74 | | 0.878 |
| 1.00 | 0.352 | 0.990 | 0.135 | 0.208 | 0.052 | 0.418 | 2.1 | 0.605 | 0.836 |
| 2.00 | 0.401 | 0.999 | 0.051 | 0.261 | 0.056 | 0.264 | 2.01 | 0.742 | 0.792 |
| 10.00 | 0.449 | 1.049 | 0.0475 | 0.280 | −0.010 | 0.054 | 1.5 | 0.960 | 0.594 |
| 100.00 | 0.450 | 1.056 | 0.0101 | 0.300 | −0.0006 | 0.0001 | 1.54 | 1.005 | 0.0101 |
| 100.00 | 0.455 | 1.055 | 0.010 | 0.300 | | | 1.31 | | |

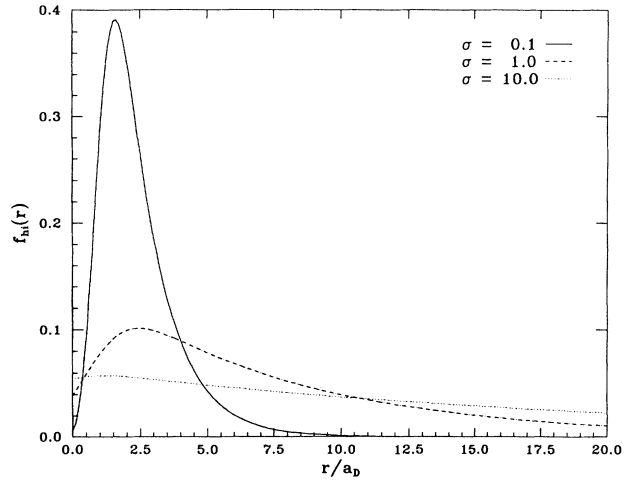


FIG. 2. The variational hole-ion Jastrow correlation function $f_{hi}$, for three different mass ratios: dotted line, $\sigma=0.1$; dashed line $\sigma=1.0$; solid line, $\sigma=10.0$.

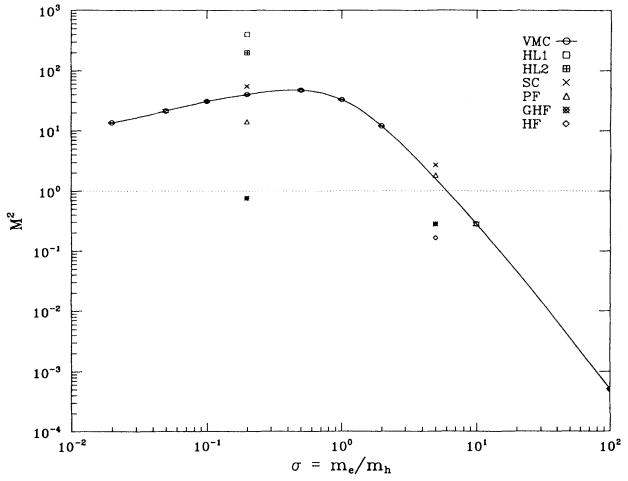


FIG. 3. The square of the $D^0X$-$D^0$ overlap integral plotted as a function of electron-hole mass ratio $\sigma$. Overlaps using other wave-function forms are plotted, including the generalized Heitler London (HL1), Ref. 39, with the hole-ion correlation (HL2), Ref. 40, the donor-exciton model of Sanders and Chang (SC), Ref. 8, 35-term Page-Fraser (PF), Ref. 9, generalized Hartree-Fock (GHF) and Hartree-Fock (HF), both from Ref. 8.

with attractive exponential behavior at large $r_{hi}$ but a significant drop-off inside the donor radius.

The scaling behavior of the hole coordinate in the large-$\sigma$ limit can be obtained from the adiabatic form of the trial wave function [Eq. (3)], $\psi(\mathbf{r}_1,\mathbf{r}_2,\mathbf{r}_h)=\psi_{\mathrm{H}^-}(\mathbf{r}_1,\mathbf{r}_2)\exp(-k_{hi}^{*}r_h)$. Including the contributions of all correlation functions involving the hole, one obtains $k_{hi}^{*}=k_{eh}^{X}+k_{eh}^{\mathrm{out}}+k_{hi}$, using the asymptotic form $f_{\alpha\beta}(r)=\exp(-k_{\alpha\beta}r)$ for the correlation functions. The effective hole orbital parameter $k_{hi}^{*}$, listed in Table II, is an indicator of the onset of the adiabatic regime, approaching for $\sigma>10$ the value of the inverse Bohr radius $a_D^{-1}/\sigma$ of a hydrogenic system with reduced mass $\sigma^{-1}$. The measured expectation value of the hole radius $\langle r_{hi}\rangle$ shown in Table I tends to the hydrogenic result of $1.5k_{hi}^{-1}$ in a similar fashion.

It is also interesting to note the large statistical error in the measured value for $r_{hi}$ in this regime, about 10% at $\sigma=100$. This is due to the disparity in scale between the $D^-$ core characterized by energies of the order of $E_D$, with a standard deviation $\sigma_E$ of about $0.1E_D$, and that of the hole with an energy that vanishes as $E_D/\sigma$, causing hole expectation values to be influenced by fluctuations in the electron coordinates. Similar problems of scale separations are at present a major bottleneck in the Monte Carlo studies of large-$Z$ atoms.[36] In our case, the worst problems occurred in the optimization of variational parameters for $\sigma<100$, whereas using an adiabatic wave function without further optimization obtained similar results, with much less statistical error.

### B. Overlap integral

The overlap integral for the donor BE is shown as a function of the electron-hole mass ratio $\sigma$ in Fig. 3. For large $\sigma$, the overlap drops to zero sharply as a consequence of the rapidly decreasing overlap of the hole with the $D^-$ core. The overlap of the hole and the electrons increases dramatically as $\sigma$ is decreased, with the onset of strong excitonic correlation between the outer electron and hole. It reaches a peak value of about 50 near $\sigma=0.4$. The slow drop off of the integral as $\sigma$ tends to zero is a result of the gradual reduction of the region of motion of the hole with increasing mass. In the limit $\sigma\rightarrow\infty$, the requirement that the hole and electron be at the same point in space at recombination results in an overlap integral proportional to the probability that the hole is at the origin. This probability scales as $\sigma^{-3}$ for a $1s$ hydrogen orbital with radius $a\sim a_D\sigma$. In the regime $\sigma\sim 0$, the overlap reduces to a constant factor due to the electron coordinates times $|\int d^3r f_{hi}(\mathbf{r})|^2/\int d^3r|f_{hi}(\mathbf{r})|^2$, which scales as $\sigma^{1/4}$ for a hole-ion correlation function of width $\sim a_D\sigma^{1/2}$ as $\sigma\rightarrow 0$. Scaling behavior is observed in the Monte Carlo data for large $\sigma$; on the other hand, the overlap scales roughly as $\sigma^{1/2}$ for $\sigma<0.1$, perhaps indicating that the system is not sufficiently in the adiabatic limit for the $\sigma^{1/4}$ behavior to be dominant.

Estimates of the expected distance from the ion at recombination of the recombining electron-hole pair and the residual donor electron are shown in Table III. These are calculated from

$$\langle r_i\rangle=\frac{\langle I|r_i|F\rangle}{\langle I|F\rangle}\ , \tag{33}$$

using an interpretation of $\psi_I(\mathbf{r}_1)\psi_F(\mathbf{r}_1,\mathbf{r}_2,\mathbf{r}_2)$ as a probability distribution for the mixed expectation values. The values for the distance of the residual electron are all roughly 1.5, the expectation value of $\langle r\rangle$ in the donor ground state. This indicates, as one would expect, a strong overlap of the average probability amplitude for the nonrecombining electron with the $1s$ donor ground state at recombination. The electron-hole pair distance

TABLE III. Logarithm of the optical overlap integral as function of electron-hole mass ratio. Also shown are the average distances from the ion at recombination of the donor electron $r_1$ and the recombining electron-hole pair $r_2$ calculated as a mixed expectation value of the overlap matrix element [Eq. (33)] as a function of electron-hole mass ratio $\sigma$. Estimated errors in parentheses.

| $\sigma$ | $\log_{10}\lvert\langle I\rvert F\rangle\rvert^2$ | $r_1$ | $r_2$ |
|---|---|---|---|
| 0.02 | 1.134(06) | 1.493(06) | 1.914(10) |
| 0.05 | 1.329(24) | 1.508(08) | 2.33(05) |
| 0.10 | 1.489(14) | 1.521(06) | 2.90(06) |
| 0.20 | 1.605(14) | 1.518(10) | 3.57(04) |
| 0.50 | 1.679(20) | 1.524(08) | 4.91(10) |
| 1.00 | 1.516(08) | 1.536(07) | 6.05(03) |
| 2.00 | 1.076(04) | 1.557(09) | 6.48(05) |
| 10.00 | −0.556(14) | 1.567(12) | 6.74(05) |
| 100.00 | −3.291(05) | 1.572(17) | 7.06(06) |

at recombination varies from somewhat larger than the hole-ion radius at $\sigma=0.02$ to roughly twice the radius of the $D^-$ core shell of the bound exciton at $\sigma=100$. It is important to note that the particle configurations of the bound exciton important to the recombination process are quite different from those that contribute to the energy, as this affects the reliability of the variational wavefunction for describing the matrix element.

### C. Error analysis and discussion

There are three basic sources of error in the VMC calculation of the optical-matrix element. Two derive from the limitations of statistical noise generated in Monte Carlo methods, and can in some sense be measured and controlled. The other stems from using a variationally obtained wave function instead of the ground-state eigenfunction in calculating the optical overlap matrix element. In contrast to the calculation of the variational energy, which is an upper bound to the true ground-state energy, the systematic errors involved with the use of a variational wave function in the overlap integral are difficult to assess and require closer analysis of the variational model used to obtain a qualitative idea of their importance.

The problem with a variational overlap matrix element is essentially that the variationally optimized ground-state wave function is not an optimal wave function for calculating the overlap integral. The variational method guarantees that $\psi$ will be optimized to match the ground state most accurately for those configurations where $|\psi(\mathbf{r}_1,\mathbf{r}_2,\mathbf{r}_3)|^2$ is large and which thus contribute most to the energy expectation value, while the integration of $\psi(\mathbf{r}_1,\mathbf{r}_2,\mathbf{r}_2)\exp(-r_1)$ may involve sizable contributions from configurations for which $|\psi^2|$ is small, and therefore poorly optimized.[16] An example in the present case would be the contribution to the overlap of configurations in which the recombining electron-hole pair is far from the donor. A comparison of the average electron and hole radii in Table I and the average electron-hole radius at recombination in Table III suggests that for $\sigma>1$, such asymptotic configurations might be expected to dominate the overlap. The overlap integral thus provides a much more strict test of the accuracy of one's variational model than the ground-state energy, and calculations that provide qualitatively reasonable binding energies may fail to provide even the order of magnitude of the overlap.

In order to gain some insight into our results, it is interesting to compare them with those of other variational models. Variational calculations to date for the BE can be divided into two general classes. Those based on a generalized Hartree Fock approach, i.e., a linear combination of single-particle orbitals [Eq. (31)] are appropriate for a $H^-+h$ complex or the large-$\sigma$ regime in the present calculation. These include the generalized Hartree-Fock calculation (GHF) of Ref. 8 and the Page-Fraser form (PF), which includes additional contributions from a Taylor series expansion in interparticle distance coordinates $r_{ij}$.[9] Wave function used to model the $\sigma<1$ regime use wave functions appropriate for the $H_2$ molecule, typically generalizations of the Heitler-London model. These include the donor-exciton model of Sanders and Chang (SC), [Eq. (11)] or those of Ungier, Suffczynski, and Adomowski in Refs. 37 (HL1) and 38 (HL2), which are similar in spirit to Eq. (32), but with a cruder treatment of hole-ion correlations. Overlap integrals from these variational calculations have been plotted for selected values of $\sigma$ along with the current calculation in Fig. 3. For the case $\sigma=0.2$ overlap estimates can be clearly grouped according to these two approaches and vary over several decades in magnitude from 0.758 for the GHF calculation to 500 for the HL1 result.

Several general characteristics of these two classes of wave functions can, in principle, explain this dramatic range in overlaps. The GHF approach ignores electron-hole correlations entirely, resulting in an overlap an order of magnitude smaller than any other model. The Page-Fraser form of Ref. 9 includes correction terms up to third order in the expansion in interparticle correlations, making up much of this underestimate. Nevertheless, the electron-hole correlations in this system are nonperturbative, including short-range cusps and the long-range excitonic correlation. It is reasonable to expect that any perturbative approach to electron-hole correlations would produce an underestimate of the overlap for low $\sigma$.

In contrast, the Heitler-London approach generally produces a high estimate of the overlap for $\sigma<1$. Large electron-hole correlations are built explicitly into the model, giving an accurate estimate of the overlap between electron and hole coordinates. The extremely large overlaps, on the order of 200 to 500 for the HL1 and HL2 wave functions, result from the insufficient inclusion of hole-in correlation. For low $\sigma$ and correspondingly low hole zero-point motion, the wave function of the hole is confined to a narrow region about the bond radius and the neglect of this correlation leads to a considerable overestimate of the optical-matrix element integral over the center of mass of the recombining electron-hole pair. The present calculation and the SC model incorporate such correlations but nevertheless can be considered as overestimates of the overlap, as the hole motion of the

variationally optimized wave functions has been found to be too diffuse.[8] The excitonic correlations that are built into the model cause a natural bias towards large exciton-donor radii, where the Heitler-London model is, in principle, exact, and away from the bonding region, where short-ranged many-body correlations are important. It seems therefore, that short of an exact treatment any attempt to cure the wave function of insufficient electron-hole overlap may lead to a corresponding overestimate of the volume of recombination of the electron-hole pair. Nevertheless the current calculation and the PF result should provide approximate upper and lower bounds to the overlap, limiting its peak value to between 14 and 40.

For $\sigma \gg 1$, where electron-hole correlations are not important, the PF wave function should be the most accurate approximation to the ground state to date. It produces an overlap that is somewhat larger than the current calculation.

The role of the electron-hole and hole-ion correlations can similarly account for the relative success of our seven-parameter calculation in calculating the BE binding energy as compared to Page-Fraser calculations. As shown in Fig. 1, the 35-term calculation achieves a superior binding energy for the regime of $\sigma > 1$ but shows relatively poor convergence at lower $\sigma$. This result is not surprising considering that the exponential hole-ion orbital used in the PF model, and the perturbative treatment of electron-hole correlations are appropriate for the large-$\sigma$ limit but poorly fit the sharply peaked hole-ion correlation and the excitonic effects which characterize the opposite limit, so that a model with fewer parameters which includes these effects might be expected to be competitive in this regime. A recent extension of this calculation to 70 parameters[18] improves the convergence of the Page-Fraser model for low $\sigma$, but again fails at around $\sigma = 0.1$.

As to the errors in our calculation associated with the Monte Carlo method, the obvious source is the statistical error in estimating an integral using a finite number of sample points. The size of this error is of order $N^{-(1/2)}$ and can be roughly estimated by measuring the standard deviation of ten or more independent repeats of the calculation. Errors of around 0.1% of the total energy were obtained in this fashion after 10 000 independent-energy evaluations. For the overlap and normalization integrals used to calculate the optical-matrix element, the standard deviation depends on the quality of the auxiliary importance wave function used, vanishing as the importance wave function tends to the actual trial wave function. Of the two importance wave functions used [Eqs. (31) and (32)], the second clearly most resembles the actual trial wave function and its use limited statistical error to about 0.3% for a 10 000 configuration run. The simpler generalized Hartree form for the importance function, with wave-function parameters chosen to reproduce the variational expectation values for particle radii $\langle r_{ei} \rangle$ and $\langle r_{hi} \rangle$, has errors on the order of 3–5 % for the same length run. Apparently, the excitonic correlations present in the more complicated form have a strong effect on the variance. The two estimates agreed with each other within the error of the cruder estimate, as expected for a properly functioning algorithm.

The second source of statistical error is the imprecision of the determination of the variational minimum using a statistical method of evaluating integrals. The method of correlated estimates used to determine the optimal variational parameters is designed to reduce much of the error in calculating the differences in energy of trial wave functions near the variationally optimal one; nevertheless one ultimately relies on the minimization of a trial energy estimated with a finite set of configurations rather than calculated exactly as an analytic integral, and thus there will be some error in determining the minimum. This optimization error can be quite large for the overlap since given a small error in the wave function $\delta\psi$ the energy near its variational minimum feels effects of order $\delta\psi^2$ while the error in the overlap will be of the order of $\delta\psi$ itself. Thus a wave function minimized to a tolerance of 0.1% in the energy could produce an overlap varying by a few percent from that of the true variational minimum. As a result, the Monte Carlo error in calculating the matrix element for any one choice of trial wave function, roughly 0.3% with the importance functions used, was generally much smaller than the errors caused by the uncertainty in determining the optimal one.

To estimate the size of the optimization error, the trial wave function was optimized for two or three different random walks. This gives a rough estimate of the precision with which the optimal wave-function parameters can be determined as the optima will vary with the random walk used. Separate calculations of the overlap matrix element with each set of variational parameters then give a crude estimate of size of the corresponding fluctuations.

## V. COMPARISON TO EXPERIMENT

The effective-mass prediction for the $A^0X$, corresponding to $\sigma > 1$ in the present calculation, is that the binding energy of the exciton should be roughly six percent of the acceptor ground-state energy for shallow acceptors within a wide range of electron-hole mass ratios. This is basically the energy required to ionize the outer hole from the $A^+$-like core of $A^0X$, with the ionization energy of the weakly bound outer electron playing a largely negligible role. In contrast, $D^0X$ complexes should show a more pronounced dependence on electron-hole mass ratio, with the binding energy reaching up to one third of the donor energy in the adiabatic limit.

Table IV compares the spherical effective-mass binding energies and those measured experimentally for several direct-gap semiconductors. The effective-mass results are in fair agreement with experimental data for donor complexes, recovering about two thirds of the experimental energy for most of the materials. Acceptor binding energies seem to be 50% or less of the experimentally observed values with a wide range in the quality of agreement. Taking into account a possible 15% increase in binding energy from the improvement of our variational wave function, this leaves roughly 20% of the donor BE and 40% of the acceptor BE binding energies unaccount-

TABLE IV. Bound exciton binding energies (in meV) of various direct-gap semiconductors. Shown are effective-mass values from various sources for donor, acceptor, and exciton binding energies, experimental electron effective mass, and hole mass and electron-hole mass ratio determined from $m_e$ and the ratio of $E_{D^0}$ and $E_{A^0}$, and binding energies of $D^0X$ and $A^0X$ in units of $E_{D^0}$ and $E_{A^0}$, and in meV. Experimental BE binding energies shown in parentheses.

| Crystal | $E_{D^0}$ (meV) | $E_{A^0}$ (meV) | $E_x$ (meV) | $m_e$ | $m_h$ | $\sigma$ | $\frac{E(\sigma)}{E_{D^0}}$ | $W_{D^0X}$ (meV) | $\frac{E(1/\sigma)}{E_{A^0}}$ | $W_{A^0X}$ (meV) |
|---|---|---|---|---|---|---|---|---|---|---|
| GaAs | 5.72[a] | 25.8[a] | 4.2[b] | 0.067[b] | 0.30 | 0.22 | 0.128 | 0.73 (0.9)[b] | 0.056 | 1.5 (2.6)[b] |
| InP | 7.24[a] | 41.0[a] | 5.1[c] | 0.077[b] | 0.44 | 0.17 | 0.144 | 1.02 (1.56)[d] | 0.056 | 2.3 (3.7)[d] |
| ZnSe | 26.1[e] | 63,65[e] | 19.0[c] | 0.16[c] | 0.39 | 0.41 | 0.099 | 2.59 (5.6)[f] | 0.057 | 3.6 (10.5)[f] |
| ZnTe | 18.7[g] | 60,63,74[g] | 13.2[c] | 0.13[c] | 0.44 | 0.31 | 0.116 | 2.14 (3.3)[h] | 0.057 | 3.4 (6.2)[h] |
| CdSe | 19.5[g] | 83,110[g] | 15.7[c] | 0.13[c] | 0.55 | 0.24 | 0.125 | 2.43 (3.2)[i] | 0.057 | 4.7 (8.2)[i] |

[a] *Numerical Data and Functional Relationships in Science and Technology,* edited by O. Madelung, Landolt-Börnstein, New Series, Group III, Vol. 22, Pt. b (Springer-Verlag, Berlin, 1982).
[b] See a, Group III, Vol. 17, Pt. a.
[c] See a, Group III, Vol. 22, Pt. a.
[d] Rühle and Klingenstein, Ref. 40.
[e] Dean *et al.*, Ref. 3.
[f] Steiner and Thewalt, Ref. 14.
[g] See a, Group III, Vol. 17, Pt. b.
[h] Schmid and Dean, Ref. 2.
[i] Minami and Era, Ref. 13.

ed for in the spherical effective-mass model.

The effective-mass theory used in this paper is expected to be especially applicable to the donor and its associated complexes, because of the very light and nearly isotropic mass of the electron (0.067 in GaAs, 0.13 in CdSe) and large dielectric constants (12 in GaAs and 9 in CdSe). The resulting donor radius $a_D$ is around 100 Å in III-V and 40 Å in II-VI semiconductors, consistent with the assumptions of the theory. Greater problems with the spherical effective-mass theory should arise with the choice of a spherical hole mass to model the degenerate and anisotropic valence-band maximum of most semiconductors. In particular for $A^0X$, shorter length scales $\sim\sigma a_D$ lead to non-negligible central cell corrections and the splitting of the valence band into heavy- and light-hole bands at nonzero wavelengths.[39] In addition, an accurate treatment of the $A^0X$ complex should include the role of $j$-$j$ coupling between holes, a problem that does not occur between the hole and the electron spin singlet of the $D^0X$ ground state. These neglected effects may account for the large variation in the quality of agreement of experimental $A^0X$ binding energies and spherical effective-mass results.

In this paper, we have used one value for $m_h$, given by the relation

$$\frac{E_{A^0}}{E_{D^0}}=\frac{m_h}{m_e}\ , \tag{34}$$

which is probably best suited for the $A^0X$ complex. An alternate choice of $m_h$ from

$$\frac{E_{D^0}}{E_X}=1+\frac{m_h}{m_e} \tag{35}$$

gives electron-hole mass ratios roughly 50% smaller with a 10% effect on $D^0X$ binding energies. The disagreement between the two estimates indicates the importance of central cell corrections and short-range spin-orbit coupling terms in the acceptor energy as compared to the exciton energy.

Radiative lifetimes for donor and acceptor bound excitons are shown in Table V. We obtain lifetimes of roughly 10–20 ps for donor bound excitons and several hundreds of picoseconds for acceptor bound excitons. The agreement with experimental data is fair for the acceptor case, comparable to that of the binding energy, whereas experimental $D^0X$ lifetimes are two orders of magnitude larger than those obtained theoretically. In the acceptor case, it should be noted that the lifetime which varies as $(1/\sigma)^3$ is quite sensitive to the value of the hole effective mass; for example, a hole mass of 0.5 for GaAs, as used in Ref. 8, gives a lifetime of 0.95 ns rather than 0.27 ns. The acceptor lifetime should be sensitive as well to significant corrections to the spherical effective-mass approximation.

The donor bound exciton lifetime is in unexpectedly poor agreement with experiment, particularly given the good fit of the experimental binding energies and the expectation that the spherical effective-mass model with an accurate variational wave function should provide a fairly realistic description of the donor bound exciton system. Finkman, Sturge, and Bhat[5] have suggested that the

TABLE V. Energy gap $E_g$, refractive index $n$, Bloch state overlap matrix element $P^2$, overlap matrix elements and radiative lifetimes of donor and acceptor BE's for various direct-gap semiconductors. Experimental lifetimes are shown for comparison below calculated ones, with errors in parentheses.

| Crystal | $E_g$ (eV) | $n$ | $P^2$ (eV) | $\sigma$ | $M^2(\sigma)$ | $\tau_{D^0X}$ (nsec) | $M^2(1/\sigma)$ | $\tau_{A^0X}$ (nsec) |
|---|---|---|---|---|---|---|---|---|
| GaAs | 1.519[a] | 3.63[a] | 25.7[b] | 0.22 | 41.0 | 0.011 | 1.80 | 0.270 |
| | | | | | | 0.75(15)[c] | | 1.0(1)[c] |
| InP | 1.424[a] | 3.46[a] | 20.4[b] | 0.17 | 37.8 | 0.018 | 1.03 | 0.670 |
| | | | | | | 0.5[d] | | 1.5[d] |
| ZnSe | 2.820[a] | 2.61[e] | 20[f] | 0.41 | 46.0 | 0.010 | 7.79 | 0.060 |
| | | | | | | 0.050(10)[g] | | 0.360[g] |
| ZnTe | 2.394[a] | 2.68[h] | 20[f] | 0.31 | 43.7 | 0.012 | 3.98 | 0.130 |
| | | | | | | 0.59[i] | | Li: 0.80(3)[i] |
| | | | | | | | | P: 0.98(4)[i] |
| CdSe | 1.842[e] | 2.45[a] | 20[f] | 0.24 | 41.7 | 0.018 | 2.89 | 0.270 |
| | | | | | | 0.51(5)[j] | | 0.80(5)[j] |

[a] *Numerical Data and Functional Relationships in Science and Technology,* edited by O. Madelung, Landolt-Börnstein, New Series, Group III, Vol. 22, Pt. a. (Springer-Verlag, Berlin, 1987).
[b] P. Lawaetz, Phys. Rev. B **4**, 3460 (1971).
[c] Finkamn, Sturge, and Bhat, Ref. 15.
[d] U. Heim, Ref. 11.
[e] See a, Group III, Vol. 17, Pt. b.
[f] Rough estimate [see, e.g., B. Segall and D. T. F. Marple, in *Physics and Chemistry of II-VI Compounds,* edited by M. Aven and J. S. Prener (North-Holland, Amsterdam, 1967), p. 336].
[g] Steiner and Thewalt, Ref. 14.
[h] B. Ray, *II-VI Compounds* (Pergamon, Oxford, 1969), p. 84.
[i] Schmid and Dean, Ref. 2.
[j] Minami and Era, Ref. 13.

long experimental lifetimes are the result of the thermal population of a large number of low-lying rotational excited states of the donor complex. In particular the $L=1$ heavy-hole rotator state in GaAs lies only 0.05 meV away from the ground state,[40] so that a significant percentage of the total bound exciton population would occupy this and higher angular momentum states at temperatures ($\sim 1-2$ K) at which most experimental data is taken. In this situation emission rates depend on a temperature-dependent oscillator strength $f_{\text{emission}}(kT)=g_{\text{BE}}/g_{\text{BE}}(kT)f_{\text{emission}}(0)$, with $g_{\text{BE}}(kT)=\sum_i \exp(-\Delta E_i/kT)$, where $\Delta E_i$ is the difference between the energy of the $i$th excited state and ground state of the bound exciton. The effect of nonzero temperature is to increase the lifetime proportion to the number of angular momentum states occupied, as the population of initial states over which the oscillator strength is averaged has increased with no additional contribution to the total oscillator strength due to optical selection rules. In contrast, the donor BE absorption coefficient, associated with the creation of an exciton at an impurity site should not show strong temperature dependence because the gap between the impurity ground state and excited states is on the order of the impurity Rydberg (6 meV in GaAs). The absorption process is thus a much more accurate experimental realization of the zero-temperature conditions assumed in calculations of the BE oscillator strength to date. The detailed balance equation [Eq. (10)] relating the two processes at finite temperature is given by

$$f_{\text{emission}}(kT)=\frac{g_I}{g_{\text{BE}}(kT)}f_{\text{abs}} \ . \tag{36}$$

The effective bound exciton degeneracy $g_{\text{BE}}(kT)$ for GaAs was estimated in Ref. 15 using this relationship and experimentally measured donor bound exciton lifetime and integrated absorption coefficients. Their measured value of $75\pm 20$, at a temperature of 3 K, might plausibly result from the population of heavy-hole rotational levels of up to $L=5$, and gives an experimental indication of the importance of thermal effects on the lifetime. In particular, the integrated absorption coefficient for the donor bound exciton line is GaAs was reported to be $3.8\pm 9\times 10^{-11}$ cm. Using the definition of the absorption coefficient in Eq. (9) and the values for the material properties and the optical-matrix element of GaAs listed in Table V, we obtain the estimate of $2.1\times 10^{-11}$ cm, which is in substantial agreement with the experimental value, as compared to the lifetime estimate shown in Table V.

Rotator state data have also been observed in InP and ZnSe. Most notably, the lowest-lying ZnSe donor BE excited state has been observed to be 0.7 meV above the ground-state energy, almost as large a gap as the entire GaAs donor BE binding energy, with other lines between 2.5 and 4.5 meV.[3] In this case then, one expects little thermal population of excited states, and thus no lifetime broadening. In fact the theoretical lifetime for ZnSe of 0.010 ns is in substantially better agreement with the

measured value of 0.050 ns than that for the other materials. The observed rotator spectrum of InP involves $L=1$ states at around 0.25 and 0.70 meV, with relative intensities as a function of temperature well fit by the assumption of thermal equilibrium at the observed exciton gas temperature.[40] The lifetime has unfortunately only been observed with the phase-shift method[11] which tends to overestimate the lifetime to some degree.[13]

## VI. CONCLUSION

We have calculated the ground-state energy and radiative oscillator strength of the exciton bound to a shallow impurity in a direct-gap semiconductor. By using an approach that systematically includes all pair correlations, and using the variational Monte Carlo method to calculate the integrals, we can obtain accurate binding energies for all mass ratios with only a few well chosen variational parameters. In particular, with the inclusion of excitonic effects, we obtain the best known variational energies to date for small electron-hole mass ratios. We have also presented arguments as to the systematic errors present in current calculations of the oscillator strength of these systems, and can qualitatively account for the relative sizes of estimates using several different variational theories; from this we conclude that the true optical-matrix element is probably bounded by our present calculation and that of Stebe and Munschy.[9] It thus appears that the great discrepancy between theoretical and experimental results for donor bound exciton lifetimes will not be significantly alleviated by a more exact theoretical calculation. Comparison with experimentally observed donor BE lifetimes in ZnSe and GaAs and the GaAs donor BE absorption coefficient is consistent with the hypothesis that much of this discrepancy is due to lifetime broadening associated with the thermal occupation of donor BE rotator states, observed in materials where these are sufficiently low lying. It should be interesting to estimate the energy levels of low-lying rotator states for several semiconductors for which data are available, and the present theory can be extended to treat the lowest-lying nonrigid rotator state with a given angular momentum $J$. In addition further experimental results, particularly of the absorption coefficient, or of the dependence of the lifetime on very low temperatures or stress could confirm the role of rotator states in determining donor bound exciton lifetimes.

## ACKNOWLEDGMENTS

We would like to thank D. Citrin and M. Ramsbey for fruitful discussions on the bound exciton lifetime, and V. J. Pandaripandhe and D. Lewart for much advice and assistance with computer algorithms. This work was supported by the Office of Naval Research (ONR) under Contract No. N00014-89-5-1157. We acknowledge the use of the Cray Research, Inc. X-MP/48 computer at the National Center for Supercomputing Applications at the University of Illinois, and the computing facilities of the University of Illinois Materials Research Laboratory.

[1]K. Cho, Opt. Commun. **8**, 412 (1973).
[2]W. Schmid and P. J. Dean, Phys. Status Solidi B **110**, 591 (1982).
[3]P. J. Dean *et al.*, Phys. Rev. B **23**, 4888 (1981).
[4]D. C. Reynolds *et al.*, Phys. Rev. B **28**, 3300 (1983).
[5]E. I. Rashba, Fiz. Tekh. Poluprovodn. **8**, 1241 (1974) [Sov. Phys. Semicond. **8**, 807 (1974)].
[6]G. C. Osbourn and D. L. Smith, Phys. Rev. B **20**, 1556 (1979).
[7]E. I. Rashba and G. E. Gurgenishvili, Fiz. Tverd. Tela (Leningrad) **4**, 1029 (1962) [Sov. Phys. Solid State **4**, 759 (1962)].
[8]G. D. Sanders and Y. C. Chang, Phys. Rev. B **28**, 5887 (1983).
[9]B. Stebe and E. Munschy, Solid State Commun. **43**, 841 (1982).
[10]C. J. Hwang, Phys. Rev. B **8**, 646 (1973).
[11]U. Heim, Phys. Status Solidi B **48**, 629 (1971).
[12]C. H. Henry and K. Nassau, Phys. Rev. B **1**, 1628 (1970).
[13]F. Minami and K. Era, Solid State Commun. **53**, 187 (1985).
[14]T. Steiner and M. L. W. Thewalt, Solid State Commun. **56**, 933 (1985).
[15]E. Finkman, M. D. Sturge, and R. Bhat, J. Lumin. **35**, 235 (1986).
[16]S. Chandrasekhar, Astrophys. J. **100**, 176 (1944).
[17]B. Stebe and E. Munschy, Solid State Commun. **35**, 557 (1980).
[18]M. Suffczynski and I. Wolniewicz, Phys. Rev. B **40**, 6250 (1989).
[19]Y. K. Ho, Phys. Rev. A **17**, 1675 (1978).
[20]D. M. Ceperley and M. H. Kalos, in *Monte Carlo Methods in Statistical Physics,* edited by K. Binder (Springer-Verlag, Berlin, 1979).
[21]D. M. Ceperley, Phys. Rev. B **18**, 3126 (1978).
[22]D. M. Ceperley and B. J. Alder, Phys. Rev. Lett. **45**, 566 (1980).
[23]P. A. Whitlock *et al.*, Phys. Rev. B **19**, 5598 (1979); M. A. Kalos, *ibid.* **24**, 115 (1981).
[24]D. M. Ceperley and B. J. Alder, J. Chem. Phys. **81**, 5833 (1984).
[25]K. E. Schmidt and J. W. Moskowitz, J. Chem. Phys. **93**, 4172 (1990).
[26]C. J. Umrigar, K. G. Wilson, and J. W. Wilkins, Phys. Rev. Lett. **60**, 1719 (1988).
[27]M. A. Lee, P. Vashishta, and R. K. Kalia, Phys. Rev. Lett. **51**, 2422 (1983).
[28]A. C. Cancio and Y. C. Chang, Phys. Rev. B **42**, 11 317 (1990).
[29]D. L. Dexter, in *Solid State Physics,* edited by F. Seitz and D. Turnbull (Academic, New York, 1958), Vol. 6, p. 361.
[30]The process involving the hole's recombination with the donor electron contributes only an additional 10% to the total oscillator strength (Ref. 8).
[31]N. Metropolis, A. Resenbluth, M. Rosenbluth, A. H. Teller, and E. Teller, J. Chem. Phys. **21**, 1087 (1953).
[32]W. L. McMillan, Phys. Rev. **138**, A442 (1965).
[33]H. James and A. S. Coolidge, J. Chem. Phys. **1**, 825 (1933).
[34]R. K. Wehner, Solid State Commun. **7**, 457 (1969). To derive the zero-point motion of the BE hole from that of two protons in $H_2$, the $H_2$ value has been scaled by a factor of $\sqrt{1/2}$.
[35]C. L. Pekeris, Phys. Rev. **112**, 1644 (1958).

[36]B. L. Hammond, P. J. Reynolds, and W. A. Lester, Phys. Rev. Lett. **61**, 2312 (1988).
[37]W. Ungier, M. Suffczynski, and J. Adamowski, Solid State Electron. **21**, 1365 (1978).
[38]W. Ungier, M. Suffczynski, and J. Adamowski, Phys. Rev. B **24**, 2109 (1981).
[39]A. Baldereschi and N. O. Lipari, Phys. Rev. B **8**, 2697 (1973); **3**, 439 (1971).
[40]W. Rühle and W. Klingenstein, Phys. Rev. B **18**, 7011 (1978).